

TEST OF ELECTRON HEAT DIFFUSIVITY AGAINST THE ELECTRON TEMPERATURE GRADIENT TURBULENCE MODEL AND INVESTIGATION OF CRITICAL TEMPERATURE GRADIENT ON TORE SUPRA

G.T. Hoang, C. Bourdelle, X. Garbet, T. Aniel, M. Ottaviani

Département de Recherches sur la Fusion Contrôlée. Association EURATOM-CEA.

13108, St Paul-lez-Durance, France

W. Horton, P. Zhu

Institute for Fusion Studies, The University of Texas at Austin, Austin, Texas 78712, USA

So far, considerable progress has been made in understanding anomalous ion transport both experimentally and computationally. In contrast, the quasi-steady state plasmas ($20 - 120 \times \tau_E$) produced in Tore Supra with dominant electron heating provide an opportunity to study electron transport under conditions similar to the burning fusion reactor in a tokamak configuration. Previously, two electron transport models have been tested against the Tore Supra results [1]:

i) Bohm-like Taroni [2] : $c_e^{Taroni} = 0.33q^2 a \frac{\nabla p_e}{p_e} \frac{T_e}{B}$ (Eq.1)

ii) offset-linear Rebut-Lallia-Watkins (RLW) [3]:

$$c_e^{RLW} = c_e^{neo} + c_e^{an} \left(1 - \frac{(\nabla T_e)_c^{RLW}}{\nabla T_e} \right) H \left(1 - \frac{(\nabla T_e)_c^{RLW}}{\nabla T_e} \right) H(\nabla q)$$

where $c_e^{an} = 2 \sqrt{\frac{T_e}{T_e + T_i}} \left(1 - \sqrt{\frac{r}{R}} \right) \frac{1}{B\sqrt{R}} \frac{q^2}{\nabla q} \left(\frac{\nabla T_e}{T_e} + 2 \frac{\nabla n}{n} \right)$ (Eq.2), $(\nabla T_e)_c^{RLW} = \frac{6}{q} \sqrt{\frac{h_j B^3}{n T_e^{1/2}}}$ (Eq.3),

It was found that the Taroni model can simulate the experimental results with some restrictions. It cannot reproduce the magnetic shear (s) effect and exhibits a disagreement in electron temperature gradient dependence ($\nabla T_e > 5-6$ keV / m). In contrast, the anomalous RLW term is better to simulate the temperature gradient and magnetic shear effects. However, the plasma parameter dependence in $(\nabla T_e)_c^{RLW}$ formula is not correctly described. In recent work [4], we analyzed a database (41 shots) of ^4He plasmas heated by fast wave (direct electron heating, FWEH) in a scenario without any ion cyclotron resonance layer. These hot electron plasmas ($T_e > 2 \times T_i$), in which the amount of RF power (P_{RF}) coupled to the electrons is more than 90% of the injected, are characterized by negligible electron-ion collisional coupling. The dataset was compiled with P_{RF} ranging from 2 MW to 7.5 MW, $I_p = 0.4 - 0.8$ MA, at central densities $n_e(0) = 5 - 7.5 \times 10^{19} \text{ m}^{-3}$ and two values of toroidal magnetic field $B = 2.2 \text{ T} / 2.8 \text{ T}$. The RF power deposition profile computed with the PION code [5] is exponentially localized inside $r/a = 0.4$. The electron thermal conductivity from the power balance analysis, with the database of 41 shots, was tested against the ETG turbulence models of electron thermal conductivity :

i) the electrostatic turbulent

$$c_e^{es} = C_e^{es} q^n \left(\frac{R}{L_{Te}} \right)^{3/2} \left(\frac{r_e^2 v_e}{T_e} \right) (|\nabla T_e - (\nabla T_e)_c|) \quad (\text{Eq. 4}), \text{ where } (\nabla T_e)_c = 1.88 \left(\frac{|\nabla T_e|}{qR} \right) \left(1 + Z_{eff} \frac{T_e}{T_i} \right) \quad (\text{Eq.5})$$

ii) the electromagnetic turbulent revised version, based on electromagnetic turbulence driven

by ETG and collisionless electron skin depth [6] $c_e^{em} = C_e^{em} q^v \frac{c^2}{w_{pe}^2} \frac{v_e}{(L_{Te} R)^{1/2}}$ (Eq.6)

Fig. 1 shows two distributions from the two sets of coefficients for various values of C_e^{es} , C_e^{em} and v . Here, we determine both the constants C_e^{es} , C_e^{em} , with various values of v , for each of the independent time slices distributed over different shots of the database, by

minimizing the square deviation between the model diffusivities and the ones obtained from power balance transport analysis. The minimum of relative deviation is obtained with C_e^{es} , C_e^{em} around 0.1 and at low value of ν , indicating a weak dependence on q for both electrostatic and electromagnetic cases. Moreover, the electromagnetic turbulence model seems to be better for the turbulent electron thermal diffusivity modeling than the electrostatic one. Indeed, the relative deviation of the electromagnetic case (20%) is lower than the electrostatic one for all values of ν .

In Fig. 2 we present an example of predictive simulations with the electromagnetic model, using the best fitted coefficients.

This figure shows that the model overpredicts the electron temperature in the outer part of the plasma ($r/a = 0.7$), which gives a predicted value of electron energy content higher than the measured value by about 15%. Simulations also show a weak difference between two cases, with and without the critical gradient of Eq. 5. This is probably due to the fact that the electron temperature gradients in our database are much higher than the predicted critical values, as shown in Fig. 3.

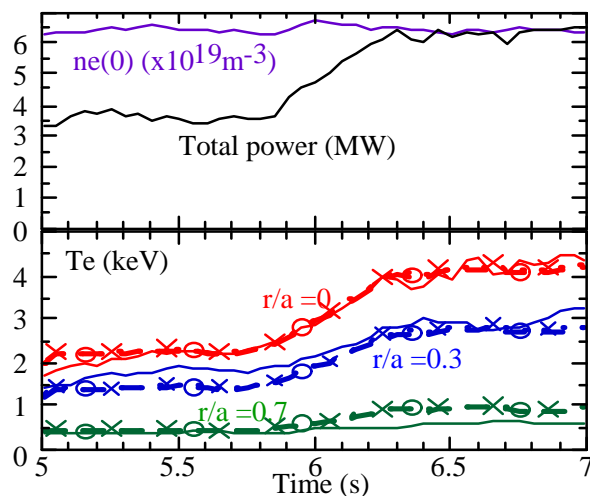


Fig. 2: Simulation of shot #TS18368 using the electromagnetic model with (dash/circle) and without (dot/cross) the critical gradient term, measurements (full). Investigation of experimental critical electron temperature has been done with a limited dataset, carefully chosen in order to obtain similar plasma parameters. These plasmas, which exhibit the same density and q profiles ($n_e(0) = 6 \times 10^{19} \text{ m}^{-3} \pm 10\%$, $q_{\text{edge}} = 4.4 \pm 5\%$), were obtained at $I_p = 0.65$ MA, $B = 2.2$ T and $P_{RF} = 1.5 - 7.4$ MW; 18 time slices of 8 ^4He discharges were selected. Power balance analysis of these FWEH discharges clearly shows the existence of a critical electron temperature gradient $(\nabla T_e)_c$, as illustrated in Fig. 4, where the electron heat flux is plotted as a function of the electron temperature gradient. We limit our analysis to the region $0.2 < r/a < 0.7$, since the plasma center is dominated by the heating source and the edge temperature measurements are affected by large uncertainties. A best

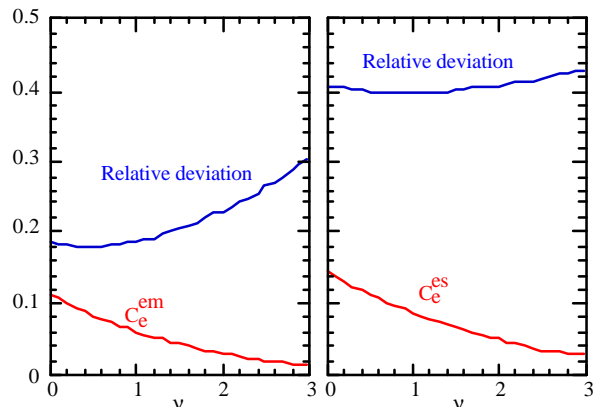


Fig. 1: Variation of fitted coefficients C_e^{es} , C_e^{em} versus ν for electromagnetic (left) and electrostatic (right) ETG models from 41 shots.

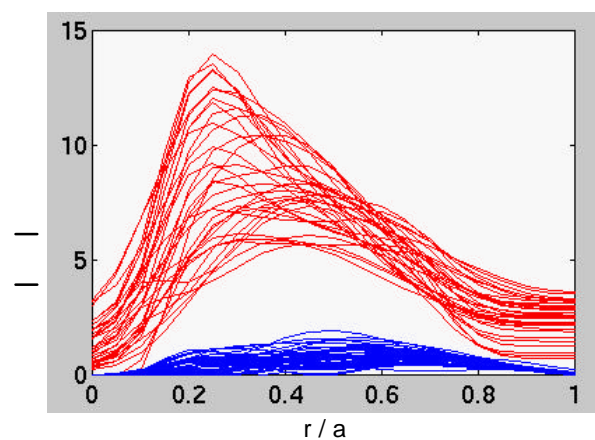


Fig. 3: Electron temperature gradient compared with the critical values of Eq.2.

linear fit gives a value of $(\nabla T_e)_c$ around 2.5 keV / m. The radial profile of $(\nabla T_e)_c$ is shown in Fig. 5, together with the theoretical critical gradients, RLW and ETG. This figure shows that the experimental result exceeds the theoretical gradient threshold by a factor of about 2. Moreover, the RLW empirical formula gives a radial profile increasing from the center to the edge which disagrees with the trend of the experimental profile. In contrast, the ETG profile appears closer to the experimental one.

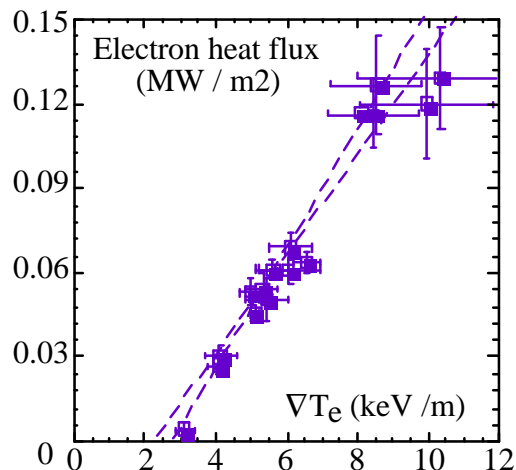


Fig. 4: Electron heat flux as a function of electron temperature gradient at mid-radius.

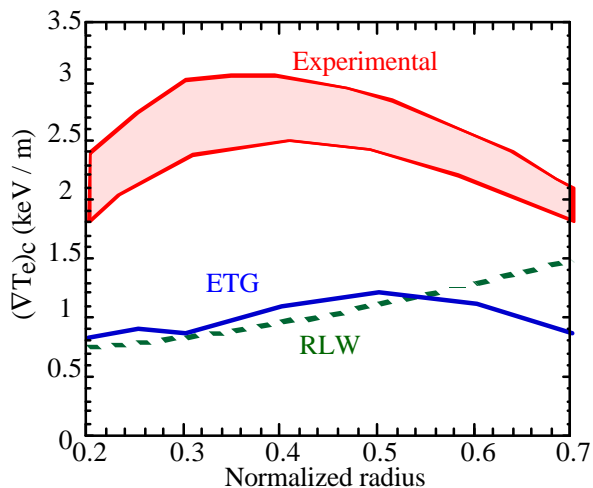


Fig. 5: Radial profile of critical gradient from power balance analysis, compared with the models.

The critical threshold is more pronounced in $\nabla T_e / T_e$ dependence, as shown in Fig. 6. Stability analysis results, with a linear electrostatic gyro-kinetic code [7] taking into account both passing and trapped electrons and ions (ITG, ETG, TEM), also confirm this trend. The results are in reasonable agreement with the power balance analysis in the outer region $0.5 < r/a < 0.7$. Fig. 7 indicates that the critical thresholds of $\nabla T_e / T_e$ deduced from both the maximum growth rates and the electron heat flux are very similar.

Moreover, the critical value $(L_{Te})_c$ ($L_{Te} = T_e / \nabla T_e$) deduced from the heat flux analysis, is found to decrease linearly with the ratio s/q , as shown in Fig. 8. A best fit of the data gives $(L_{Te})_c = 0.23 \frac{s}{q}$, corresponding to $\frac{R}{(L_{Te})_c} \approx 10 \frac{q}{s}$ ($R = 2.28$ m, being the major radius). Fig. 8

also shows a fair agreement between the transport and stability analyses. For comparison, the ETG critical threshold is reported. By multiplying Eq. 5 by a factor of 2, we obtain a reasonable agreement with the experimental results, except in the core region ($r/a < 0.3$) where its value is overestimated. This could be explained by the uncertainties in the determination of s and q .

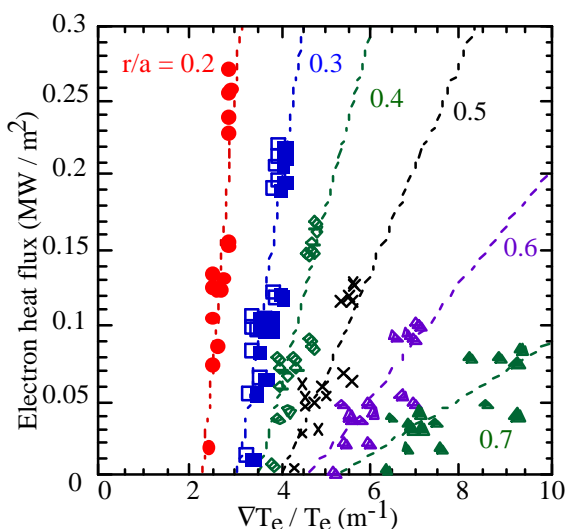


Fig. 6: Electron heat flux versus $\nabla T_e / T_e$, at different radii, from a dataset of 18 time slices of 8 discharges, with the same parameters.

In summary, a critical electron temperature gradient exists clearly in Tore Supra hot electron plasmas. Its value is almost twice higher than the theoretical models (RLW, ETG given in Eq. 5). The ETG model predicts a profile similar to the experimental one. The dimensionless parameter $\frac{R}{(L_{Te})_c} \frac{s}{q}$ deduced

from transport analysis is about 10, which is in good agreement with stability analysis results. The ETG electromagnetic turbulent revised model [6] seems to be better for the electron transport modeling. However, the electron heat flux versus the temperature gradient could be

fitted by either offset-linear or strong power fit. This could be the reason why all the models, with weak (Taroni, RWL, electromagnetic turbulence) or strong (electrostatic turbulence) dependence in ∇T_e , can simulate electron transport with reasonable discrepancies when ∇T_e exceeds the critical value.

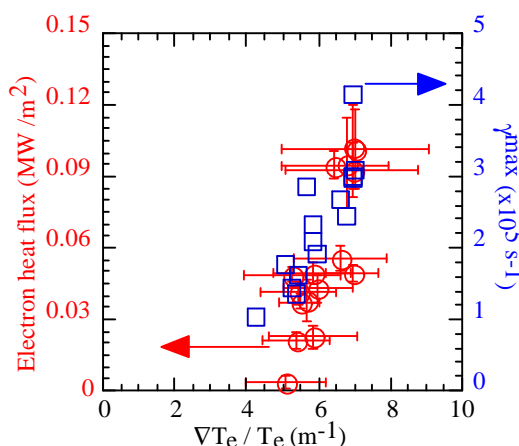


Fig. 7: Electron heat flux (circles) and maximum growth rates (squares) versus $\nabla T_e / T_e$ at $r/a = 0.6$.

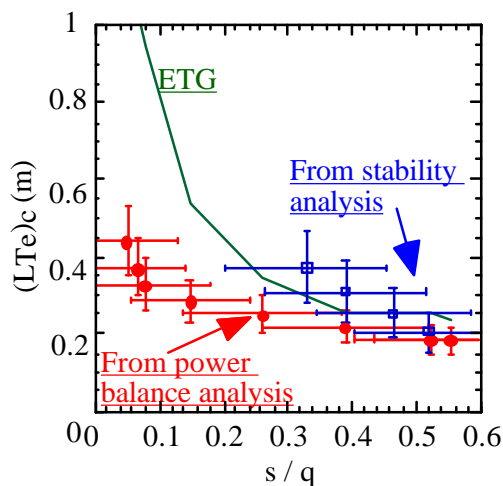


Fig. 8: $(L_{Te})_c$ from power balance (circles) and stability (squares) analyses versus the ratio s/q . $(\nabla T_e)_c$ in Eq. 5 is multiplied by 2.

References

[1] G.T. Hoang et al., Nucl. Fusion Vol 38, (1998) 117.	[4] W. Horton et al., Phys. Plasmas , 7, (2000) 1494.
[2] A. Taroni et al., 20 th EPS conference, (1993).	[5] L.-G. Eriksson et al., Nucl. Fusion 33 (1993) 1037.
[3] P.H. Rebut, et al., Phys. Fluids B3 (1991) 2209.	[6] W. Horton, Reviews of Mod. Phys 71 (1999) 735.
	[7] C. Bourdelle et al., this conference.